

INDUCTANCE DETERMINATION OF INTERIOR PERMANENT MAGNET SYNCHRONOUS MOTOR CONSIDERING SATURATION

*Rodkin D., student, *Zinchenko O., student, *Peresada S., prof., **Kiselychnyk O., prof.

**Igor Sikorsky Kyiv Polytechnic Institute, department of automation of electromechanical systems and electric drives, **University of Warwick, UK*

Introduction. Interior permanent magnet synchronous motors (IPMSMs) found their application in high-performance drives because of high power density, high torque/inertia ratio, high reliability and high-power factor. Especially that motor type can be used in electric vehicles (EVs) and robotics application due to its small size and high efficiency.

Due to its benefits IPMSM are used for high precision and dynamic applications. Control algorithms for this purpose are usually based on a motor model and require the values of motor parameters for proper functionality. It is well known that most of IPMSMs are designed to have a high saliency ratio between motor inductances along two axes [1]. Because of saliency, saturation effects of the machine are very distinct. Saturation effects cause parameters to vary nonlinearly, especially inductances along two axes, making huge impact on the control performance. Therefore, determination of the inductances along d- and q-axis is a task to be solved.

Different approaches can be used to determine machine inductances. Finite element analysis (FEA) used in [2] and [3] where data was saved into look-up tables. Some researchers use estimation methods to determine inductances in d-q frame [4] – [6]. In [4] root least square (RLS) method was used. Authors in [5] approximated flux linkage data obtained from FEA by a function in a form of multivariable polynomial. Online inductance estimation based on discrete dynamic motor model is used in [6]. In [7] inductances as functions of corresponding currents are determined in steady state considering core losses. In [8] d – and q – axis fluxes are evaluated from series of tests in standstill. After that inductances are determined from flux as functions of both currents.

Purpose. To determine inductances along d- and q-axis of IPMSM in stand still while motor is fed by inverter and compare different methods to obtain inductance dependences on self-currents along each axis considering saturation effects.

Material of the research. Interior permanent magnet synchronous motor can be modelled in rotor reference frame also called d-q reference frame [9]. In order to increase accuracy of inductance determination, rotor of the motor is locked during the tests in different positions. In stand still voltage equations of IPMSM will look

$$\begin{aligned} L_d \frac{di_d}{dt} &= -Ri_d + v_d, \\ L_q \frac{di_q}{dt} &= -Ri_q + v_q, \end{aligned} \tag{1}$$

where (v_d, v_q) – voltages along d- and q-axis, (i_d, i_q) – currents along d- and q-axis, R – stator windings resistance, L_d and L_q – inductances along d- and q-axis.

Test description. Inductances L_d and L_q can be determined from tests depending on relative rotor position to an applied voltage vector. The main idea was taken from [10].

Experimental scheme is presented in fig. 1. Phase to phase voltage and current in phase A are measured using differential probes and oscilloscope. Voltage is measured directly, current - from current sensor output resistor. Idea of the test is to observe current and voltage during transients from active state to zero state, where states are:

1. Active positive state. +DC voltage is applied to phase A and –DC to B and C phase. In this case transistors VT1, VT4 and VT6 are opened.
2. Active negative state. -DC voltage is applied to phase A and +DC to B and C phase. In this case transistors VT2, VT3 and VT5 are opened.
3. Zero state. All transistors are closed

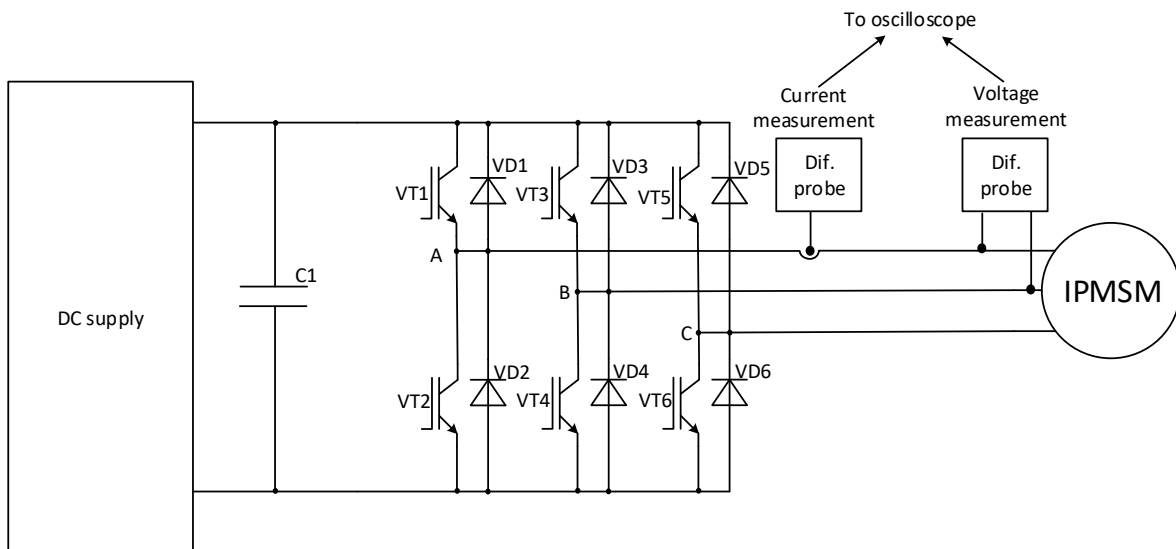


Figure 1 – Experimental scheme

In rotor reference frame d-axis is aligned with magnets. In order to measure inductance L_d , d – axis has to be aligned with phase A voltage vector (fig. 2). In order to set rotor position, +DC voltage is applied to phase A and –DC to B and C phase. After that rotor has to be locked. As for flux weakening, loss minimisation and maximum torque per ampere control implementation d – axis current is negative, only transient from active negative state to zero state is considered.

In order to measure inductance L_q , d – axis has to be orthogonal to phase A voltage vector (fig. 3). Rotor alignment can be done by means of

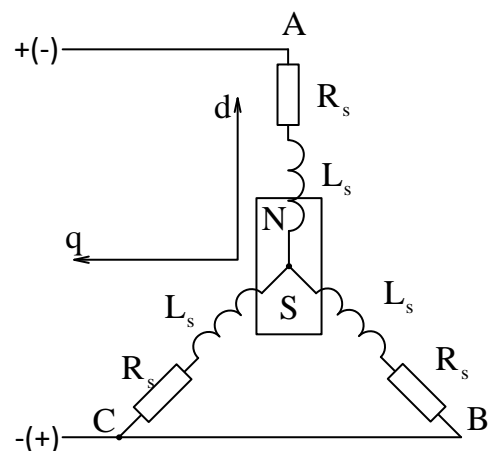


Figure 2 – D-axis configuration

applying +DC voltage to phase B and –DC voltage to phase C (transistors VT3 and VT6 are opened). After rotor is locked transients from active states to zero state are considered.

One of the features of inductors is to maintain smooth current flow. During operation in active states, inductances store energy by means of creating magnetic field. Once system decays to zero state, all energy stored in inductances is used to continue currents flow inducing voltage that is bigger than DC supply voltage and with opposite polarity. Current starts to flow through the diodes until it falls to zero. It means that all energy stored in inductances is dissipated. For instance, before transition, transistors VT1, VT4 and VT6 are opened. After state change all transistors are closed, and current starts to flow through the diodes VD2, VD3 and VD5. Transients are shown in fig. 4. From fig. 4 it is easily seen that voltage changes its polarity, and its amplitude is bigger than applied voltage in active state.

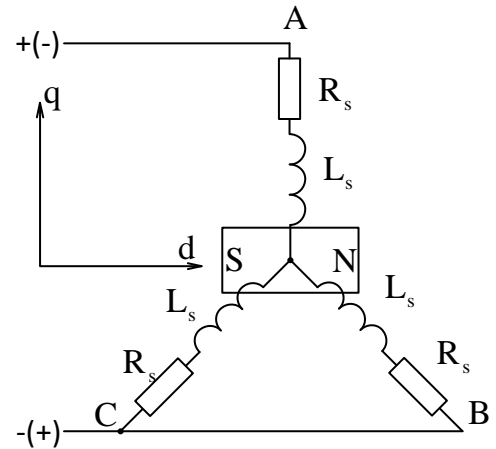


Figure 3 – Q-axis configuration

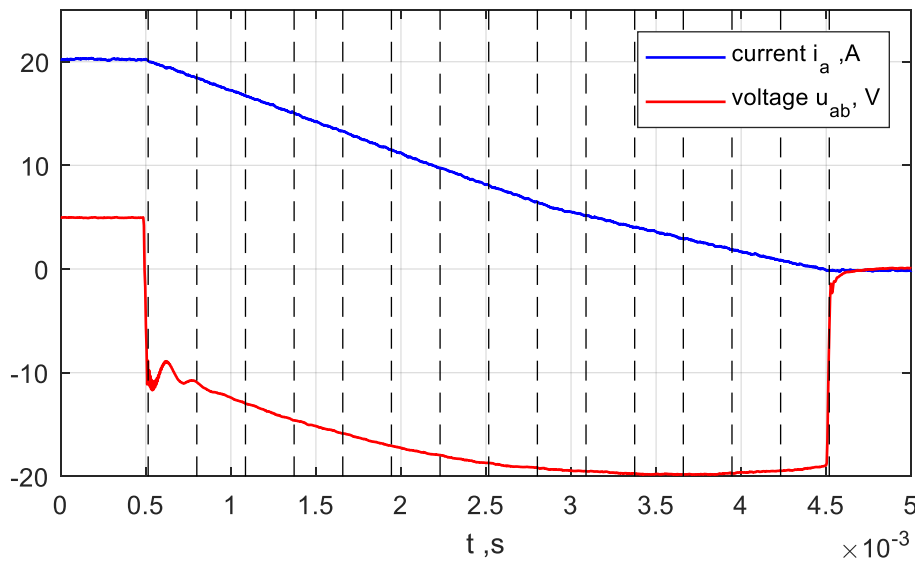


Figure 4 – Current and voltage transients

It should be mentioned that current in phases B and C is taken to be the same and therefore voltage drop on transistors VT4, VT6 and diodes VD3, VD5 is the same. Therefore, we can assume that B and C are directly connected, what is important for the further data analysis.

According to fig. 2-3 equivalent resistance and inductance of this circuit are $R_{eqv} = 1.5R_{ph}$, $L_{eqv} = 1.5L_{ph}$, considering that impedance in each phase is the same, where R_{ph} and L_{ph} are phase resistance and inductance.

Methods proposed below can be used to determine both d- and q – axis inductance. The only difference is a rotor position during the test.

Method 1. Directly from the model. In motionless regime IPMSM model can be presented as RL – circuit model. This model considering equivalent parameters and measured data is

$$L_{\text{eqv}} \frac{di_a}{dt} = -i_a R_{\text{eqv}} + u_{\text{ab}}, \quad (2)$$

From (2) inductance can be evaluated as

$$L_{\text{ph}}(i_a) = \frac{2}{3} \left(\frac{u_{\text{ab}} - i_a R_{\text{eqv}}}{\frac{di_a}{dt}} \right), \quad (3)$$

where u_{ab} - measured voltage between phases A and B, i_a - measured phase A current,

Conditionally transient can be divided to several segments as it is shown in fig. 4. Number of segments can be different.

Inductance according to (3) can be found on each segment. Average value of voltage and current in each segment is taken. Resistance is considered as constant and can be determined from Ohm's law from for constant values of current and voltage before transient (fig. 4). Current derivative is assumed to be constant during one segment and evaluated as change of current value during one segment divided by length of the segment.

Method 2. From flux value. In flux linkage terms RL – circuit model is

$$\frac{d\psi_{\text{eqv}}(i_a)}{dt} = -i_a R_{\text{eqv}} + u_{\text{ab}}, \quad (4)$$

where $\psi_{\text{eqv}}(i_a)$ - flux linkage.

Time derivative of the flux can be expressed as

$$\frac{d\psi_{\text{eqv}}(i_a)}{dt} = \frac{\partial \psi_{\text{eqv}}(i_a)}{\partial i_a} \frac{di_a}{dt}. \quad (5)$$

Substitution (5) in (4) gives

$$\frac{\partial \psi_{\text{eqv}}(i_a)}{\partial i_a} \frac{di_a}{dt} = -i_a R_{\text{eqv}} + u_{\text{ab}}. \quad (6)$$

Comparison (6) and (2) gives us the following way to determine inductance [11]

$$L_{\text{ph}}(i_a) = \frac{2}{3} L_{\text{eqv}}(i_a) = \frac{2}{3} \frac{\partial \psi_{\text{eqv}}(i_a)}{\partial i_a} \approx \frac{2}{3} \frac{\Delta \psi_{\text{eqv}}(i_a)}{\Delta i_a}. \quad (7)$$

Flux linkages from (4) can be determined as [8]

$$\psi_{\text{eqv}} = \int (-i_a R_{\text{eqv}} + u_{\text{ab}}) dt + C, \quad (8)$$

where $C = \text{const}$ – initial condition that is not important in this case as inductance in (7) is evaluated from change of flux but not its absolute value. Therefore C can be taken as zero.

Change of current and flux in (7) can be taken as a difference between their values in each segment in fig. 4. Another option is to approximate flux in (8) and take derivative directly.

Method 3. Iterative method. Also inductance can be determined using iterative method. The idea is following. If real inductance value satisfies condition $L(i) \in [L_{\min}, L_{\max}]$ for every values of current within operation range, then RL-circuit has to be modelled for each inductance in range $[L_{\min}, L_{\max}]$ with some step ΔL when measured voltage values are applied. During the simulation the biggest difference between simulated and measured current is detected. Inductance value for which current error is the least is expected to be the real one.

As the goal is to determine inductance as a function of current, transients can be divided to several segments as it is shown in fig. 4. System can be modelled in each segment separately. Initial condition of modelled current has to be equal to measured current in the first point of a segment.

Results. Fig. 5 shows d – and q – axis inductances as functions of corresponding currents. Determined flux in the method 2 is approximated as 3rd order polynomial. Inductance values from method 1 and 3 are approximated as 2nd order polynomial. According to the figure, all methods give almost the same result.

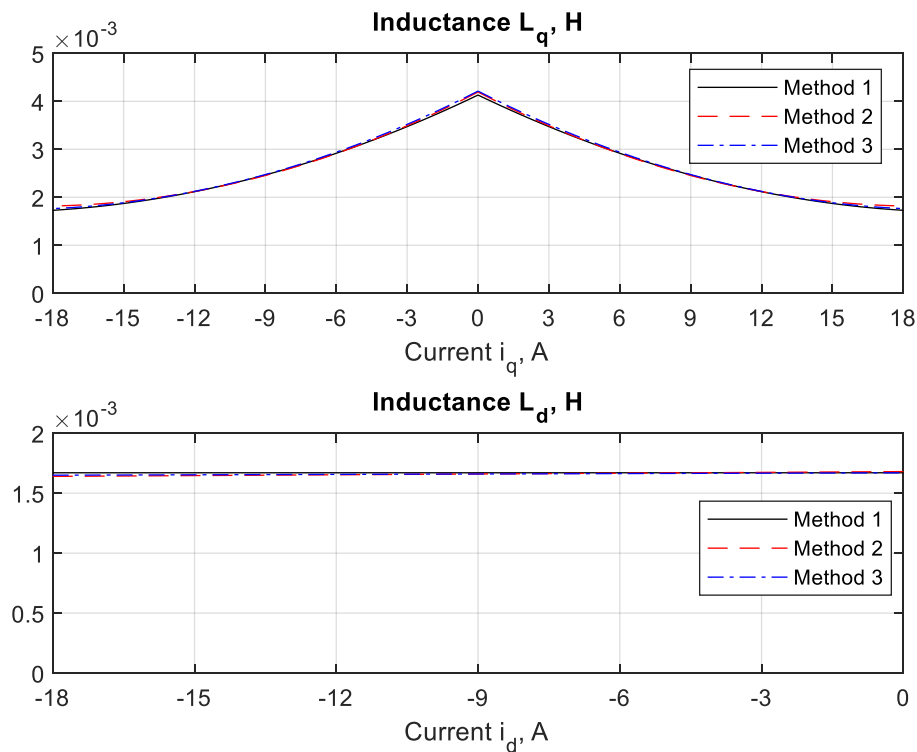


Figure 5 – d – and q – axis inductances determined with different methods

D – axis inductance value remains constant for all values of the current. Q – axis inductances decreases with absolute current value increasing. Results show variation of q-axis inductance due to saturation. At the same time variation of d-axis inductance almost absent.

Conclusion. Saturation effects in the motor with salient rotor have huge impact on overall control performance and therefore cannot be neglected in high dynamic

and precision applications. Evaluation of saturation effects can be done by means of implementing variable inductances as a functions of currents into control algorithm. In this article test description for inductance determination of the IPMSM is presented. After that inductances are determined using three different methods. Each of proposed methods allows to receive similar result.

References

1. Jeong Y. Adaptive Flux Observer with On-line Inductance Estimation of an IPMSM Considering Magnetic Saturation / Y. Jeong and S. Sul // IEEE 36th Power Electronics Specialists Conference – 2005 – P. 2467-2473.
2. Shin K., Characteristic Analysis of Interior Permanent-Magnet Synchronous Machine With Fractional-Slot Concentrated Winding Considering Nonlinear Magnetic Saturation / K. Shin, J. Choi and H. Cho // IEEE Transactions on Applied Superconductivity. – 2016. – Vol. 26. – №4. – P. 1-4.
3. Matzen T. N., Modelling magnetic saturation effects in IPMSMs for use in sensorless saliency based methods / T. N. Matzen and P. O. Rasmussen // 2007 European Conference on Power Electronics and Applications. – 2007. – P. 1-8.
4. Kim S., Torque Ripple Improvement for Interior Permanent Magnet Synchronous Motor Considering Parameters With Magnetic Saturation / S. Kim // IEEE Transactions on Magnetics. – 2009. – Vol. 45. – №10. – P. 4720-4723.
5. Jeong I., Inductance Estimation of Electrically Excited Synchronous Motor via Polynomial Approximations by Least Square Method / I. Jeong, B. Gu, J. Kim, K. Nam and Y. Kim // IEEE Transactions on Industry Applications. – 2015. – Vol. 51. – №2. – P. 1526-1537.
6. Dang D. Q., Online Parameter Estimation Technique for Adaptive Control Applications of Interior PM Synchronous Motor Drives / D. Q. Dang, M. S. Rifaq, H. H. Choi and J. Jung // IEEE Transactions on Industrial Electronics. – 2016. – Vol. 63. – №3. – P. 1438-1449.
7. Fernandez-Bernal F., Determination of parameters in interior permanent-magnet synchronous motors with iron losses without torque measurement / F. Fernandez-Bernal, A. Garcia-Cerrada and R. Faure // IEEE Transactions on Industry Applications. – 2001. – Vol. 37. – №5. – P. 1265-1272.
8. Stumberger B., Evaluation of saturation and cross-magnetization effects in interior permanent-magnet synchronous motor / B. Stumberger, G. Stumberger, D. Dolinar, A. Hamler and M. Trlep // IEEE Transactions on Industry Applications. – 2003. – Vol. 39. – №5. – P. 1264-1271.
9. R. Krishnan, Permanent Magnet Synchronous and Brushless Dc Motor Drives / R. Krishnan // CRC Press, Boca Raton. – 2009.
10. Viktor Bobek, PMSM Electrical Parameters Measurement / Viktor Bobek // Document Number:AN4680, Freescale Semiconductor, Inc. – 2013
11. Pellegrino G. The Rediscovery of Synchronous Reluctance and Ferrite Permanent Magnet Motors / Pellegrino, Gianmario & Jahns, Thomas & Bianchi, Nicola & Soong, Wen & Cupertino, Francesco. – 2016.